Research in Astron. Astrophys. **2013** Vol. **13** No. **7**, 875–884
http://www.raa-journal.org *http://www.iop.org/journals/raa*

Research in Astronomy and Astrophysics

Simulation of a ground-layer adaptive optics system for the Kunlun Dark Universe Survey Telescope

Peng Jia[1,2,3,4] and Sijiong Zhang[2,3]

[1] School of Astronomy and Space Science, Nanjing University, Nanjing 210093, China;
[2] National Astronomical Observatories / Nanjing Institute of Astronomical Optics & Technology, Chinese Academy of Sciences, Nanjing 210042, China; *sjzhang@niaot.ac.cn*
[3] Key Laboratory of Astronomical Optics & Technology, Nanjing Institute of Astronomical Optics & Technology, Chinese Academy of Sciences, Nanjing 210042, China;
[4] Key Laboratory of Modern Astronomy and Astrophysics, Ministry of Education, Nanjing 210093, China

Received 2012 May 9; accepted 2013 March 13

Abstract Ground Layer Adaptive Optics (GLAO) is a recently developed technique extensively applied to ground-based telescopes, which mainly compensates for the wavefront errors induced by ground-layer turbulence to get an appropriate point spread function in a wide field of view. The compensation results mainly depend on the turbulence distribution. The atmospheric turbulence at Dome A in the Antarctic is mainly distributed below 15 meters, which is an ideal site for applications of GLAO. The GLAO system has been simulated for the Kunlun Dark Universe Survey Telescope, which will be set up at Dome A, and uses a rotating mirror to generate several laser guide stars and a wavefront sensor with a wide field of view to sequentially measure the wavefronts from different laser guide stars. The system is simulated on a computer and parameters of the system are given, which provide detailed information about the design of a practical GLAO system.

Key words: instrumentation: adaptive optics — methods: numerical

1 INTRODUCTION

The Antarctic is considered to be one of the best places on the ground for optical and infrared astronomical observations (Lawrence et al. 2004). Dome A ($80^\circ 22'$S, $77^\circ 21'$E, 4093 m above sea level) is located on the Antarctic plateau, which is considered to be the coldest and driest area on Earth. A Chinese expedition reached Dome A in 2005 and the Kunlun Antarctic station (7.3 km southwest of Dome A) was set up in 2009. The results of testing the site for astronomical observations show that the observation conditions seem to be better in Dome A than in other sites in Antarctica. New plans for astronomy observations in Dome A have been broadly discussed, and the design of optical-infrared telescopes has also been proposed following scientific plans. The Kunlun Dark Universe Survey Telescope (KDUST) is one of the new telescopes (Stone 2010) that will be set up at the Kunlun Antarctic station.

The plan for KDUST is to perform high-resolution image surveys and precision photometry with a wide field of view (Zhao et al. 2011). As is well known, atmospheric turbulence will have an effect on the observations, especially when the telescope is working in photometry or imaging mode. The atmospheric turbulence in Dome A is mainly distributed below $15\,\mathrm{m}$ (Lawrence et al. 2006), which is lower than the height where the telescope will be set. This design will improve the seeing and ground layer adaptive optics (GLAO) can also be used to further increase image quality. GLAO (Hubin et al. 2005, Anderson et al. 2006) is different from the Conventional Adaptive Optics System (CAOS). CAOS corrects for errors induced by turbulence from different altitudes. Although the performance of CAOS is diffraction-limited, satisfactory performance is limited to a field of view of about $10''$. Generally, GLAO corrects the wavefront errors induced by ground-layer turbulence and leaves the wavefront error induced by the high-altitude turbulence uncorrected. For the atmospheric turbulence in Dome A, more than 80% of the energy in the turbulence is distributed near the ground. With GLAO, the telescope can provide good performance over a wide field of view. Section 2 describes the parameters used in the simulation and discusses some important parts of the GLAO system. Section 3 draws the conclusion of this paper.

2 GLAO FOR KDUST

KDUST has many important scientific objectives. It will help us to understand dark matter and dark energy, and will also help in the discovery of new exoplanets. The GLAO system is designed to increase the observation ability of KDUST. We simulate the GLAO system for KDUST with different sets of parameters, and evaluate the system performance with different evaluation factors under different observation goals. The simulation results show the great potential of GLAO applied to KDUST. A detailed information guide for GLAO is provided at the end of this section.

2.1 Scientific Goal of GLAO for KDUST

According to Wang[1], the scientific objectives for KDUST include: exoplanet detection, dark matter and dark energy. The observation mode for the scientific objectives is a wide field survey. According to Frieman et al. (2008), Munshi et al. (2008), Zhan et al. (2009) and Hegde & Kaltenegger (2012), the main observation results will include precise multi-color photometry and direct imaging from different bands in a wide field of view. The scientific aims determine the performance requirements of the GLAO system, and the wide field sky imaging survey needs a very uniform point spread function (PSF) over a wide field of view. The Strehl ratio is used to evaluate the PSF. The Strehl ratio is defined as the ratio of the peak intensity of the observed image to a theoretical maximum peak intensity in a perfect system. It is widely used to evaluate well–calibrated optical systems, such as telescopes and microscopes. For GLAO on KDUST, the Strehl ratio is planned to increase two to four times, and differences in the Strehl ratio for different positions in the field of view should be less than 20%. Precise photometry of quasars, supernovae and stars with exoplanets is another important scientific objective for KDUST. We will use full width at half magnitude (FWHM) to evaluate the precision of the photometry. The FWHM (full width at half maximum) is defined as the width of the celestial coordinate range where less than half of the optical power from the star is attenuated. It is planned for GLAO to decrease the FWHM to less than $0.1''$ for the whole field of view in $700\,\mathrm{nm}$.

The requirement of a uniform PSF and to decrease the FWHM to the same degree over a wide field of view is beyond the ability of a CAOS system.

The field of view of CAOS is small (about $10''$), and the image quality decreases rapidly outside the system's field of view. Meanwhile, GLAO projects a few guide stars to different areas in the sky and receives wavefronts from them. The wavefront signal is processed and sent to a deformable mirror (DM) to compensate for the wavefront errors induced by turbulence. Generally speaking, the

[1] *aag.bao.ac.cn/Academic/xian/ppt/8.19am/wang_lifan.pdf*

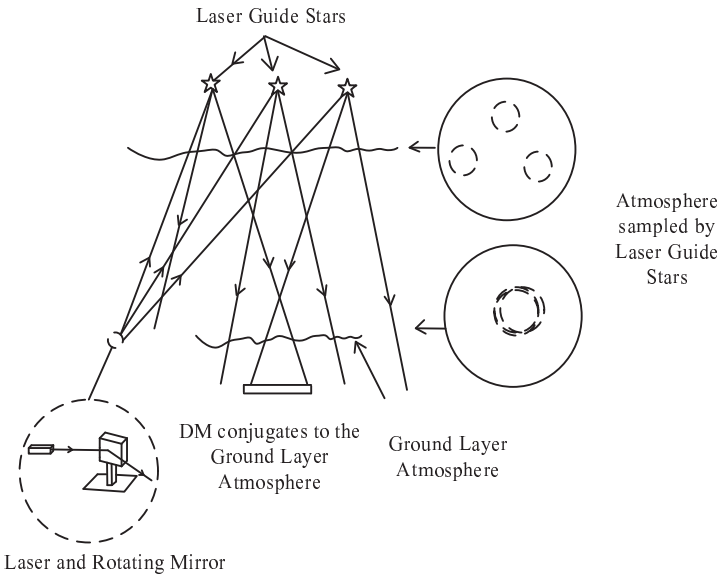

Fig. 1 Schematic diagram of GLAO for the Kunlun Dark Universe Survey Telescope.

signal sent to the DM is the average of different wavefronts. The averaged wavefront is considered to be induced by the ground layer atmospheric turbulence as shown in Figure 1. GLAO makes a moderate correction over a wide field of view. If the ground-layer turbulence has a strong effect on its whole distribution, then GLAO will significantly improve the image quality over a wide field of view (a few tens of arcsec to a few arcmin).

2.2 Parameters Describing the Atmospheric Turbulence

The performance of an adaptive optics system that depends on layers of the atmosphere, such as GLAO and multi–conjugate adaptive optics (MCAO), is strongly affected by the structure and distribution of atmospheric turbulence. Detailed parameters and distribution of the atmospheric turbulence need to be measured in different layers of the atmosphere with scientific instruments (such as microthermal sensors) installed in meteorological balloons, where layers are defined as regions at different heights. With this method, the velocity and turbulence strength distribution in the different layers can be well measured. As far as we know, the atmospheric turbulence in Dome A has not been measured using the above method.

We use the measurement results from Dome C (Trinquet et al. 2008) as our atmospheric turbulence parameters. As shown from the simulation (Lascaux et al. 2011) and results from some early measurements (Saunders et al. 2009; Bonner et al. 2010; Yang H. et al. 2010), the difference in the atmospheric turbulence between these two sites is not significant, and the atmospheric turbulence in Dome A is even less, which is better for astronomical observations.

Two sets of parameters are chosen to generate the atmospheric turbulence. A set of parameters representing the average state is used to test the performance of the system in the ordinary state, and a set of parameters representing the worst state (where the weights of the free atmosphere are large and the wind velocity is strong) is used to test the performance of the system under severe conditions (as shown in Tables 1 and 2). The simulation shows that the Strehl ratio is 0.1146 for the average state and 0.06982 for the worst state (700 nm with r_0 equal to 30 cm), and the FWHM is $0.1631''$ and $0.2407''$ for the average and worst states, respectively.

Table 1 The Parameters of the Average State of Atmospheric Turbulence

Layer	Height (m)	Weight	Wind Velocity (m s^{-1})	Wind Direction (°)
1	19	0.8904	4	139
2	170	0.068 49	7	185
3	4469	0.034 25	15	239
4	10 038	0.006 849	20	300

Table 2 The Parameters of the Worst State of Atmospheric Turbulence

Layer	Height (m)	Weight	Wind Velocity (m s^{-1})	Wind Direction (°)
1	22	0.5319	7	139
2	220	0.4184	10	185
3	4900	0.042 55	20	239
4	10 038	0.007 091	20	300

2.3 Initial Parameters of GLAO for KDUST

KDUST is an optical-infrared telescope (Yuan et al. 2013) with a diameter of 2.5 m and a secondary mirror that has a 0.625 m diameter. It will perform high spatial resolution and high depth sky surveys. The GLAO apparatus will use a rotating mirror and a laser to generate multiple laser guide stars (LGSs) by reflecting light from the laser to different areas in the field of view as the mirror rotates (Morris & Myers 2006). A wide-field Shack-Hartmann wavefront sensor will then detect the wavefronts from the different areas as shown in Figure 1.

GLAO will work in the optical-infrared bands, and the field of view will be about $20'$ (much bigger than that available from CAOS). The Strehl ratio and FWHM are used as evaluation factors for the system, and we plan to increase the Strehl ratio by more than two times and decrease the FWHM to less than $0.1''$ over the whole field of view in 700 nm. Because there are complicated relationships among the number of actuators in the deformable mirror, the number of sub–apertures in the Shack-Hartmann wavefront sensor, the number and positions of the guide stars in the sky and the correction frequencies of the system, computer simulation is important for saving costs and increasing design efficiency (Jia $\&$ Zhang 2013). The Durham extremely large telescope adaptive optics simulation platform (Basden et al. 2007) is used as our simulation platform, and a system with different parameters has been analyzed.

The GLAO system in this simulation consists of a tip-tilt mirror, a quadrant detector, a deformable mirror, a laser device, a rotating mirror, a Shack–Hartmann wavefront sensor with a wide field of view and a science camera. The initial parameters are listed in Table 3. This is a CAOS, and we will change its parameters in steps according to our requirements. Then we can develop a GLAO system that satisfies our needs. Because there are many parameters that need to be defined, the system simulation has been divided into two stages. The first is to determine the static parameters of the system. In this stage, the LGSs will be assumed to be motionless (just like multiple LGSs, which are distributed in different positions in the sky), and the overall system's working frequency is 300 Hz.

The second stage is to determine the dynamical parameters of the system. Here we analyze the frequency matching problem between the frequency of correction for the system (not including the rotating mirror) and that of the rotating mirror, and the optimal working frequency of the overall system (with the rotating mirror).

The wavelength of the LGS is 430 nm, the wavelength of the natural guide star (NGS) is 500 nm and the wavelength for the science camera is 700 nm. We will use a pair of dichroic filters to divide the light from different targets as needed.

Table 3 Parameters of the Initial System

Device	Parameters
Natural Guide Star	$5''$ to the center of the field
Laser Guide Star	No laser guide star
Quadrant detector	Ideal detector
Tip–tilt mirror	Remove the tip–tilt directly measured by the quadrant detector
Deformable mirror	11×11 actuators Gaussian profile response
Wavefront Sensors	11×11 subapertures Shack–Hartmann type
Control method	Modal method

2.4 Simulation for Different Sets of Parameters Describing GLAO

There are many parameters that affect the final system performance, and the relation between the system performance and the parameters is complicated. It is necessary to perform simulations with different sets of parameters. The initial parameters (as shown in Table 3) will be sequentially altered to satisfy the correction requirements of GLAO.

2.4.1 Number and positions of guide stars

An NGS is used to sample the tip–tilt induced by the atmospheric turbulence in this system. Its position, number and magnitude are important, but it cannot be designed. The average case for the NGS is considered in the simulation. The NGS is $30''$ to the middle of the field of view and has a magnitude of 10 in the 500 nm band.

There are two types of LGSs: the Rayleigh LGS and the sodium LGS. The Rayleigh LGS is produced by the Rayleigh scattering of the laser in the atmosphere. It is a much simpler and less costly technique, but it is only effective at a lower height compared to the sodium guide star, and it cannot sample the atmospheric turbulence at a high layer. Because the atmospheric turbulence in Dome A is mainly distributed near the ground, the error induced by the undetected atmospheric turbulence at a high layer is much less than that at ordinary sites. Considering the expense and complexity of implementing an LGS, the Rayleigh LGS is chosen for the GLAO system.

For the GLAO system, the number and positions of the LGS have an effect on the overall system performance. The LGS should be properly placed to cover the field of view. Over the field of view, the number of LGSs affects the uniformity of the PSF. Figure 2 illustrates the relation between the number of LGSs and the Strehl ratio.

GLAO in KDUST has the particular characteristic that the number of guide stars will decrease the overall system frequency, because the wavefront sensor has to sample the wavefronts from all guide stars. For this reason, the number of guide stars has to be no greater than four. The positions of the four LGSs and the NGS in GLAO for KDUST are shown in Table 4.

Table 4 LGS and NGS Positions in GLAO

Guide Star Type	Distance to the center of the field
NGS	30 arcsec
LGS a	0.5 arcmin
LGS b	2.5 arcmin
LGS c	5 arcmin
LGS d	7.5 arcmin

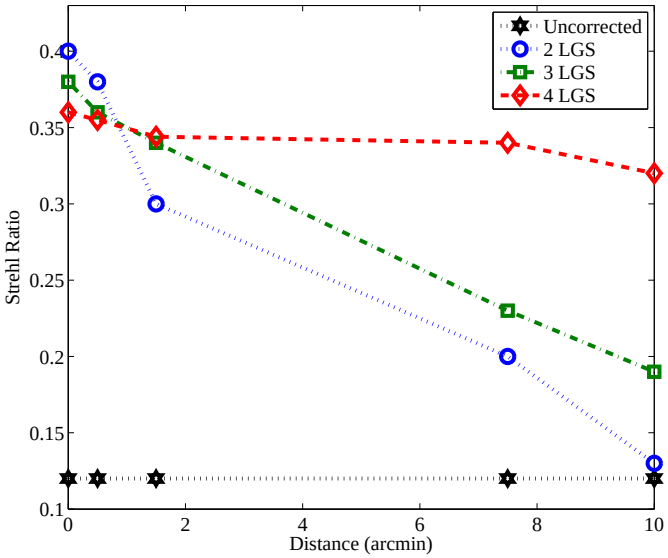

Fig. 2 Relationship between the number of LGSs and the Strehl ratios.

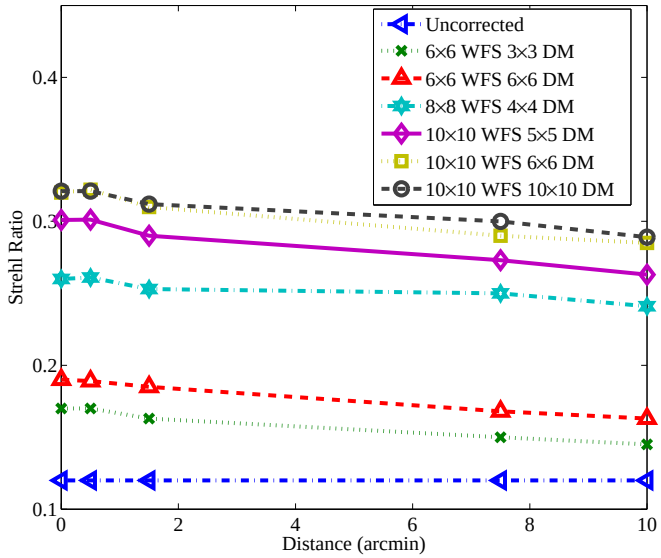

Fig. 3 Relation between the number of WFS sub-apertures and the number of DM actuators.

2.4.2 Determination of the static parameters

The GLAO control method used in this simulation is the modal control approach. The first 10 Zernike polynomials in Noll's sequential indices (Noll 1976) without pistons are corrected. The problem of

matching the number of DM actuators with the number of wavefront sensor (WFS) sub-apertures in GLAO is also considered. When the system is operating, part of the WFS may only be used to sample the wavefront and the DM used to correct the aberrations. Some of these cases are simulated as shown in Figure 3. When more than 6×6 of the WFS sub-apertures are illuminated and more than 4×4 actuators are used, the system's performance is acceptable. According to the results of the simulation, the system will use a WFS with 10×10 sub-apertures and a DM with 10×10 actuators.

2.4.3 Determination of the dynamical parameters

The LGS in this system is different from that in other GLAO systems, which makes the operation of GLAO for KDUST different from that in other GLAO systems. Ordinary GLAO systems will use three to five laser devices to point to different areas in the field of view to generate LGSs. Because the atmospheric turbulence at Dome A is distributed in the low region of the atmosphere, the isoplanatic angle and the coherent time, which are important characteristics in adaptive optics systems, are larger than those in other sites on Earth. The overall system operating frequency can be lower than that of GLAO systems in other sites. A laser device and a rotating mirror are used to generate the LGSs. There are two disadvantages of this system: the limitation of the frequency of the whole system caused by the rotating mirror, and the error introduced by the complex mechanical and control system of the rotating mirror and the LGS. Because the overall system operating frequency is lower in the GLAO system for KDUST, the deterioration in results caused by the delay in the rotating mirror are negligible within a certain range. The error introduced by the complex mechanical and control system includes the spatial domain error and time domain error. The spatial domain error is caused by the nonlinearity and drift of the rotating mirror. In real applications, the position of the LGS in each cycle will change, but this is not a serious problem. A modern rotating mirror has high resolution (about $0.2''$) and linearity (less 0.1%), and also accurate positioning of the LGS is not very important, as shown from Figure 4. The time domain error is caused by the frequency mismatch between the rotating mirror and the WFS. The measurement of the WFS and the rotation mirror should be synchronized. If they are not synchronized, the overall system performance will deteriorate.

As shown in Figure 5, the rotating mirror and the wavefront sensor will use an external trigger to keep them synchronous. The external trigger is a mature technology widely applied to the control of the instruments and it has high precision. The mismatch problem can be eliminated by a well designed external trigger circuit. Although the price of four Rayleigh LGSs is not high, it is much higher than implementing a single Rayleigh LGS with a rotating mirror which can reflect the laser light, effectively multiplying the number of available LGSs. In addition, the volume required for four LGS devices, including the electrical source and the optical bench, is hard to install in KDUST because of the limited capacity at the top of the tower, and the requirement for high electrical power for the laser device is also a problem in Antarctica.

When the system is operating, the laser will sequentially point to a few different pre–defined positions in the field of view. Then the wide field Shack-Hartmann wavefront sensor will sample the wavefronts from different LGSs. When all wavefronts from the four positions are recorded by the WFS, the DM will correct the wavefront according to the signal from the WFS.

The whole process is defined as a cycle and the flow chart of the cycle is shown in Figure 5. The relationships among the exposure time of the WFS, the time cost by the rotating mirror and the system performance are shown in Figure 6. When the overall system frequency is larger than 200 Hz, the system satisfies our needs. Because the laser has to point to four positions in a cycle, the frequency of the rotating mirror should be at least four times that of the overall system. A rotating mirror with more than one thousand Hertz is fast enough for our system. The sample rate for our WFS is at least 200 Hz, and commonly used optical components satisfy our needs.

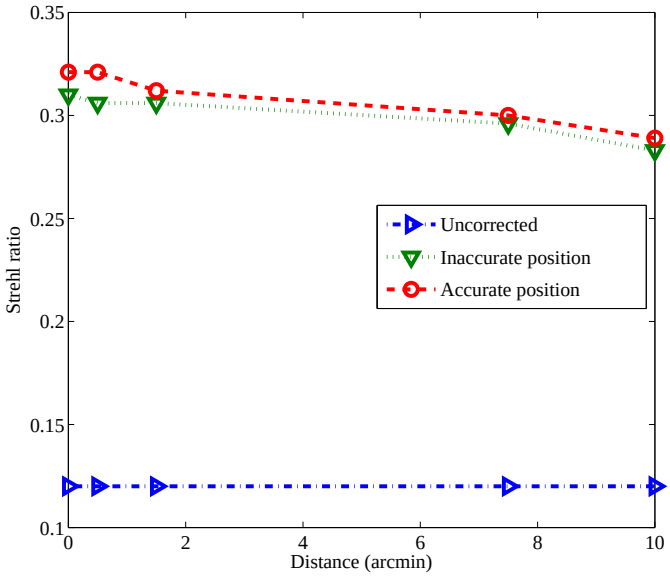

Fig. 4 The system performance when the rotating mirror has a 5% error in pointing accuracy (the LGS for each position is distributed in a $3''$ circle).

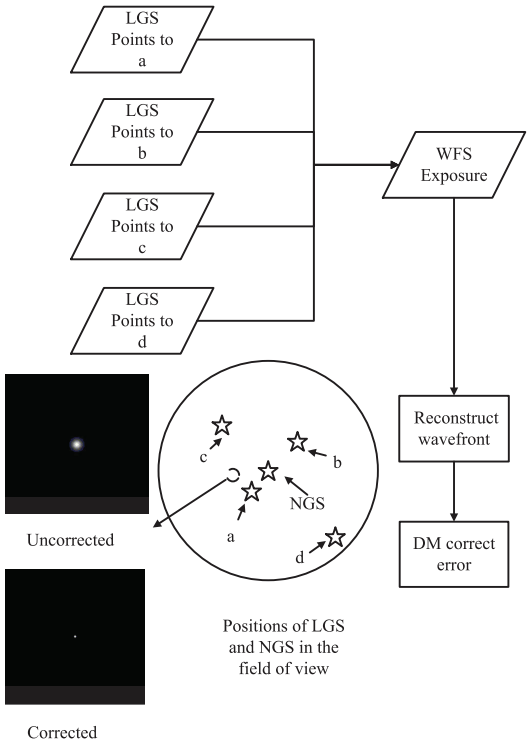

Fig. 5 The flow chart of a cycle, the pointing positions of the LGS, and a comparison between corrected and uncorrected long exposure images of one of the stars in the field of view.

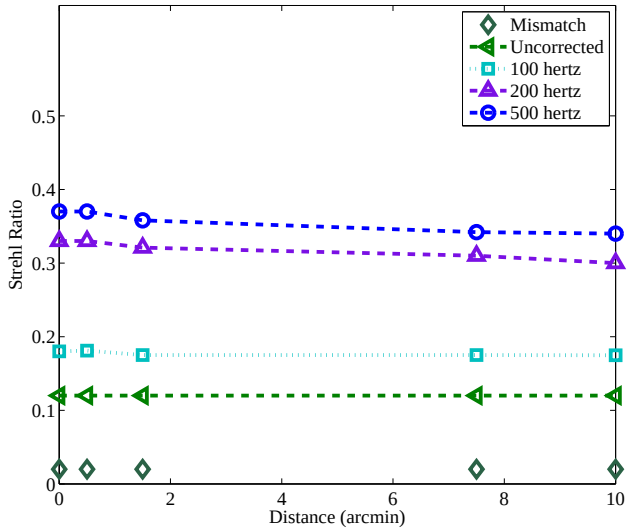

Fig. 6 System performance under different overall system frequencies. A mismatch occurs when the ratio of exposure time to the rotation time of the rotating mirror is not an integer.

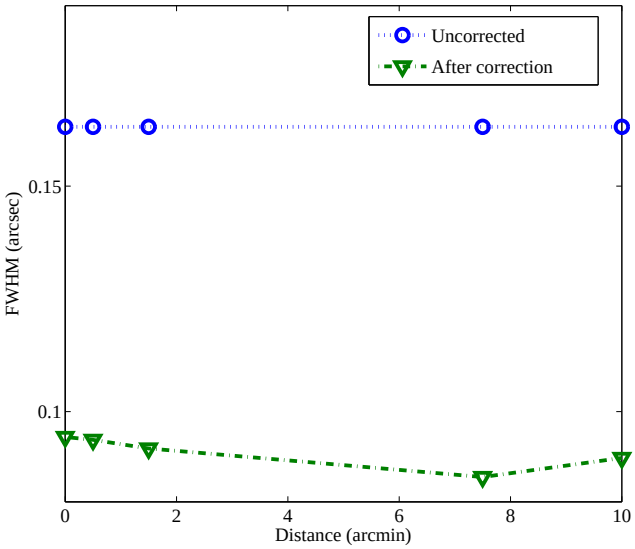

Fig. 7 The performance of the final system with FWHM as the evaluation factor.

2.5 The Performance of GLAO

The final GLAO system can increase the Strehl ratio by more than two times and decrease the FWHM to less than $0.1''$, as shown in Figure 7, over the whole field of view in 700 nm. The final system parameters are shown in Table 5.

Table 5 The Parameters of the Final System

Device	Parameters
Natural Guide	$30''$ from the center of the field
Star	magnitude 10 in 500 nm
Laser Guide	One laser guide star
Star	with a rotating mirror
Quadrant detector	Ideal detector
Tip–tilt mirror	Remove the tip–tilt directly measured by the quadrant detector
Deformable mirror	10×10 actuators Gaussian profile response
Wavefront Sensors	10×10 subapertures Shack–Hartmann type
Control method	Modal method
Overall frequency	200 Hz

3 CONCLUSIONS

The simulation of the GLAO system for KDUST shows great potential for GLAO applications with a rotating mirror and a Rayleigh LGS. This system reduces cost with only one laser device, and the deterioration in results caused by the delay of the rotating mirror are negligible within a certain range because of the unique distribution of the atmospheric turbulence in Antarctica. The problem of synchronizing the rotating mirror with the wavefront sensor, and the error contributed by the rotating mirror, are analyzed. The reconstruction method and the control method are classical methods in this simulation. Some of the new wavefront reconstruction methods and control methods will be tested and the results will be further improved by implementing the new methods.

Acknowledgements Many thanks to professor Xiangyan Yuan's helpful discussion and the reviewer's kind suggestions.

References

Andersen, D. R., Stoesz, J., Morris, S., et al. 2006, PASP, 118, 1574
Basden, A., Butterley, T., Myers, R., & Wilson, R. 2007, Appl. Opt., 46, 1089
Bonner, C. S., Ashley, M. C. B., Cui, X., et al. 2010, PASP, 122, 1122
Frieman, J. A., Turner, M. S., & Huterer, D. 2008, ARA&A, 46, 385
Hegde, S., & Kaltenegger, L. 2012, in EGU General Assembly Conference Abstracts, 14, eds. A. Abbasi, & N. Giesen, 13743
Hubin, N., Arsenault, R., Conzelmann, R., et al. 2005, Comptes Rendus Physique, 6, 1099
Jia, P., & Zhang, S. 2013, Science in China G: Physics and Astronomy, 56, 658
Lascaux, F., Masciadri, E., & Hagelin, S. 2011, MNRAS, 411, 693
Lawrence, J. S., Ashley, M. C. B., Tokovinin, A., & Travouillon, T. 2004, Nature, 431, 278
Lawrence, J. S., Ashley, M. C. B., Burton, M. G., et al. 2006, in Society of Photo-Optical Instrumentation Engineers (SPIE) Conference Series, 6267
Morris, T. J., & Myers, R. M. 2006, MNRAS, 370, 1783
Munshi, D., Valageas, P., van Waerbeke, L., & Heavens, A. 2008, Phys. Rep., 462, 67
Noll, R. J. 1976, Journal of the Optical Society of America (1917–1983), 66, 207
Saunders, W., Lawrence, J. S., Storey, J. W. V., et al. 2009, PASP, 121, 976
Stone, R. 2010, Science, 329, 1136
Trinquet, H., Agabi, A., Vernin, J., et al. 2008, PASP, 120, 203
Yang, H., Kulesa, C. A., Walker, C. K., et al. 2010, PASP, 122, 490
Yuan, X., Cui, X., Su, D., et al. 2013, in IAU Symposium, 288, 271
Zhan, H., Knox, L., & Tyson, J. A. 2009, ApJ, 690, 923
Zhao, G.-B., Zhan, H., Wang, L., Fan, Z., & Zhang, X. 2011, PASP, 123, 725